INTERNATIONAL JOURNAL FOR NUMERICAL METHODS IN FLUIDS, VOL. 14, 1009–1018 (1992)

FLUX DIFFERENCE SPLITTING FOR 1D OPEN CHANNEL FLOW EQUATIONS

FRANCISCO ALCRUDO, PILAR GARCIA-NAVARRO AND JOSE-MARIA SAVIRON

Departamento de Ciencia y Tecnologia de Materiales y Fluídos, Facultad de Ciencias, Universidad de Zaragoza, Ciudad Universitaria, Zaragoza 50009, Spain

SUMMARY

An upwind finite difference scheme based on flux difference splitting is presented for the solution of the equations governing unsteady open channel hydraulics. An approximate Jacobian needed for splitting the flux differences is defined that satisfies the conditions required to construct a first-order upwind conservative discretization of the equations. Added limited second-order corrections make the resulting scheme robust and accurate for the computation of all regimes of open channel flow. Some numerical results and comparisons with other classical schemes under exacting conditions are presented.

KEY WORDS Mathematical modelling Shock capturing Upwind schemes Flux difference splitting Open channel flow

INTRODUCTION

Mathematical simulation of hydraulic phenomena is becoming increasingly important in engineering practice since it offers the possibility of cheaply evaluating the response of hydraulic systems to a variety of practical situations. Among these, rapidly varied open channel flow possesses certain features that make it important to predict but most difficult to compute. Supercritical flows with hydraulic jumps and bores are awkward to represent even if a shock-capturing method is employed.

During the last decade much effort has been paid to the numerical solution of systems of conservation laws. This effort was mainly driven by the need for accurate and efficient solvers for the equations of compressible gas dynamics. Among the techniques developed to accurately resolve discontinuities, upwind schemes based on flux difference splitting[1,2] have been successfully applied to a wide class of problems involving the Euler equations.

One-dimensional channel flow can be described by a system of conservation laws, namely the St. Venant equations, which resemble in many respects the equations of compressible flow. Flux-difference-splitting techniques provide a means for the use of high-resolution schemes based on flux limiters. These achieve non-oscillatory solutions while retaining second-order accuracy in smooth flow regions. Glaister[3] proposed a scheme based on Roe's Riemann solver and applied it to flow in a channel of infinite width. In this paper those ideas are generalized to the more practical situation of channels with arbitrary cross-section.

0271–2091/92/091009–10$05.00

Received July 1991

EQUATIONS

It is assumed that one-dimensional flow of water in a channel of slowly varying cross-section with sufficiently gentle bottom slope can be described by the St. Venant equations.[4] They express conservation of mass and momentum and can be cast in the divergent vector form

$$\frac{\partial \mathbf{U}}{\partial t}+\frac{\partial \mathbf{F}}{\partial x}=\mathbf{G}, \tag{1}$$

$$\mathbf{U}=\begin{pmatrix} S \\ Q \end{pmatrix}, \qquad \mathbf{F}=\begin{pmatrix} Q \\ Q^2/S+gI_1 \end{pmatrix}, \qquad \mathbf{G}=\begin{pmatrix} 0 \\ G_2 \end{pmatrix}. \tag{2}$$

S is the wetted cross-section of the channel, Q is the volume flow of water and g is the acceleration due to gravity. I_1 is the hydrostatic pressure force term, which can be written

$$I_1=\int_0^h (h-\eta)\sigma(\eta)\,\mathrm{d}\eta, \tag{3}$$

where h is the water depth and $\sigma(\eta)$ is the channel width at depth η:

$$\sigma=\frac{\partial S}{\partial h}. \tag{4}$$

The source term G_2 in (2) accounts for the bed slope, the friction and the variation of the channel shape with distance. In this paper only the numerical treatment of the homogeneous part of (1) will be addressed and, accordingly, σ is assumed to be a fixed function of the depth for the entire channel. For the sake of brevity the actual form of G_2 is not given explicitly. The homogeneous part of the system is of the hyperbolic type and is responsible for most of the difficulties found when it is numerically integrated; namely, its non-linearity can give rise to discontinuous solutions currently referred to as bores or jumps.

The Jacobian matrix of the flux is

$$\mathbf{A}=\frac{\partial \mathbf{F}}{\partial \mathbf{U}}=\begin{pmatrix} 0 & 1 \\ gS/\sigma-Q^2/S^2 & 2Q/S \end{pmatrix}, \tag{5}$$

with eigenvalues and eigenvectors

$$a^{1,2}=u\pm c, \qquad \mathbf{e}^{1,2}=\begin{pmatrix} 1 \\ u\pm c \end{pmatrix} \tag{6}$$

$$u=Q/S, \qquad c=\sqrt{(gS/\sigma)}. \tag{7}$$

The eigenvalues of $\mathbf{A}$ correspond to the two characteristic speeds and therefore their signs provide information about the directions of propagation of information in the channel. With the definition of $\mathbf{A}$, an equivalent but non-divergent form of equation (1) is

$$\frac{\partial \mathbf{U}}{\partial t}+\mathbf{A}\frac{\partial \mathbf{U}}{\partial x}=\mathbf{G}. \tag{8}$$

FIRST-ORDER UPWIND SCHEME

In order to solve (1) with an explicit time-stepping scheme, the domain of integration is discretized as (x_j, t^n), where $x_j=j\Delta x$, $j=1,2,\ldots,$ and $t^n=n\Delta t$, $n=1,2,\ldots.$

For supercritical flow from left to right both characteristic speeds are positive, indicating that information can only travel downstream, so that the following first-order upwind scheme can be considered:

$$\mathbf{U}_j^{n+1} = \mathbf{U}_j^n - \lambda \Delta \mathbf{F}_{j-1/2}, \tag{9a}$$

where $\lambda = \Delta t/\Delta x$ and $\Delta \mathbf{F}_{j-1/2} = \mathbf{F}_j - \mathbf{F}_{j-1}$ is the increment of $\mathbf{F}$ across the $j-1/2$ cell interface. Conversely, for supercritical flow from right to left both characteristic speeds are negative and the same upwind scheme will read

$$\mathbf{U}_j^{n+1} = \mathbf{U}_j^n - \lambda \Delta \mathbf{F}_{j+1/2}. \tag{9b}$$

In the case of subcritical flow the two characteristic speeds are of different sign, indicating that information travels in both directions or, more precisely, that some contributions are propagating upstream while others are moving downstream. In order to construct an upwind scheme valid for all regimes and directions of flow, an appropriate decomposition of the flux related to positive and negative propagation speeds is needed. Formally one could write

$$\mathbf{U}_j^{n+1} = \mathbf{U}_j^n - \lambda \Delta \mathbf{F}_{j+1/2}^- - \lambda \Delta \mathbf{F}_{j-1/2}^+, \tag{10}$$

where $\Delta \mathbf{F}_{j+1/2}^{\pm}$ are the increments of flux associated with positive and characteristic speeds respectively across the $j+1/2$ cell interface. The decomposition should be such that for supercritical flows either $\Delta \mathbf{F}_{j+1/2}^+$ or $\Delta \mathbf{F}_{j+1/2}^-$ are zero. A suitable way of performing that splitting is addressed in the next section.

ROE LINEARIZATION

Roe[5] proposed a technique for constructing scheme (10) for the Euler equations ensuring conservation, and Glaister[3] applied the same idea to the St. Venant equations for a channel of infinite width. In this section the procedure is extended to channels of finite cross-section of arbitrary shape in order that the above first-order scheme can be applied to actual channel flow computations.

At every time level and for every pair of adjacent cells an approximate Jacobian matrix $\tilde{\mathbf{A}}$ is sought that fulfils the following properties.

(i) $\Delta \mathbf{F}_{j+1/2} = \tilde{\mathbf{A}}_{j+1/2} \Delta \mathbf{U}_{j+1/2}$.

(ii) $\mathbf{A}_{j+1/2} = \tilde{\mathbf{A}}_{j+1/2}(\mathbf{U}_j, \mathbf{U}_{j+1})$.

(iii) $\mathbf{A}(\mathbf{U}, \mathbf{U}) = \mathbf{A}(\mathbf{U}) = \partial \mathbf{F}/\partial \mathbf{U}$.

(iv) $\mathbf{A}$ has real eigenvalues with a complete set of eigenvectors.

Property (i) guarantees conservation of the scheme that relies upon $\tilde{\mathbf{A}}$, while (iii) ensures consistency with the original equation. With regard to property (iv) one searches for the matrix that has eigenvalues and eigenvectors of the form

$$\tilde{a}^{1/2} = \tilde{u} \pm \tilde{c}, \qquad \tilde{\mathbf{e}}^{1,2} = \begin{pmatrix} 1 \\ \tilde{u} \pm \tilde{c} \end{pmatrix}, \tag{11}$$

and the problem of finding $\tilde{\mathbf{A}}$ is now transferred to that of finding the average values $\tilde{u}$ and $\tilde{c}$ that meet the requirements (i)–(iv). Such values, and therefore $\tilde{\mathbf{A}}$, exist as will be shown later by construction.

Following (iv), any increment in the conserved variables $\mathbf{U}$ can be decomposed as a linear combination of the eigenvectors of $\tilde{\mathbf{A}}$:

$$\Delta \mathbf{U}_{j+1/2} = \sum_{k=1}^{2} \tilde{\alpha}^k_{j+1/2} \tilde{\mathbf{e}}^k_{j+1/2}, \tag{12}$$

and from property (i) the flux difference is expressed as

$$\Delta \mathbf{F}_{j+1/2} = \sum_{k=1}^{2} \tilde{\alpha}^k_{j+1/2} \tilde{a}^k_{j+1/2} \tilde{\mathbf{e}}^k_{j+1/2}. \tag{13}$$

This decomposition provides a means for defining the plus and minus flux increments across $j \pm 1/2$ of equation (10), i.e.

$$\Delta \mathbf{F}^{\pm}_{j+1/2} = \sum_{k=1}^{2} \tilde{\alpha}^k_{j+1/2} \tilde{a}^{k\pm}_{j+1/2} \tilde{\mathbf{e}}^k_{j+1/2}, \tag{14}$$

where $a^{\pm} = (a \pm |a|)/2$ has been used. Equation (14) guarantees what have been called plus and minus flux differences, to be related to positive and negative characteristic speeds respectively. This leads to natural upwind differencing in (10).

After some algebraic manipulations, scheme (10) with flux difference splitting (14) can be cast in conservation form as

$$\mathbf{U}^{n+1}_j = \mathbf{U}^n_j - \lambda(\mathbf{F}^*_{j+1/2} - \mathbf{F}^*_{j-1/2}), \tag{15}$$

with the following numerical flux:

$$\mathbf{F}^*_{j+1/2} = \tfrac{1}{2}(\mathbf{F}_{j+1} + \mathbf{F}_j) - \tfrac{1}{2} \sum_{k=1}^{2} \tilde{\alpha}^k_{j+1/2} |\tilde{a}^k_{j+1/2}| \tilde{\mathbf{e}}^k_{j+1/2}. \tag{16}$$

In order to calculate the value of $\tilde{u}$, $\tilde{c}$ and the $\tilde{\alpha}^k$, use is made of the vector equations (12) and (13). From (12) one gets

$$\tilde{\alpha}^{1,2}_{j+1/2} = \frac{1}{2\tilde{c}} [\pm \Delta Q_{j+1/2} + (\tilde{c} \pm \tilde{u}) \Delta S_{j+1/2}]. \tag{17}$$

Using (17) and (13), a quadratic equation for $\tilde{u}$ is found whose useful solution is

$$\tilde{u}_{j+1/2} = \frac{\sqrt{(S_j)} u_j + \sqrt{(S_{j+1})} u_{j+1}}{\sqrt{S_j} + \sqrt{S_{j+1}}}, \tag{18}$$

which is the *square root averaging* of Roe[5]. For $\tilde{c}$ one gets

$$\tilde{c}^2_{j+1/2} = g \frac{I_{1\,j+1} - I_{1\,j}}{S_{j+1} - S_j}. \tag{19}$$

When the values of two adjacent cross-sections are equal, if there is no variation of the cross-section shape along the channel, their hydrostatic pressure distribution is the same and $\tilde{c}$ is not defined by (19). By performing the limiting process, one finds the following formula for $\tilde{c}$:

$$\tilde{c}^2_{j+1/2} = \begin{cases} g \dfrac{I_{1\,j+1} - I_{1\,j}}{S_{j+1} - S_j} & \text{if } S_{j+1} - S_j \neq 0, \\ c^2_j = c^2_{j+1} & \text{if } S_{j+1} - S_j = 0, \end{cases} \tag{20}$$

which is consistent with property (iii). It is interesting to note that the approximate Jacobian so built is independent of the form of the cross-section of the channel; in other words it is well defined whatever the functional dependence of σ on h may be.

This Jacobian has the interesting property that whenever the states of two adjacent cells can be connected by a hydraulic jump, it projects only onto one eigenvector whose associated eigenvalue corresponds to the velocity of propagation of the jump.[1,5] This property makes the upwind scheme (15), (16) well suited for the computation of rapidly varied flows with the possibility of formation of bores. It has, however, the disadvantage of admitting unphysical stationary jumps (those in which energy increases across the jump). The cure to this problem is fortunately inexpensive. Among the various possibilities the easiest way is to replace the moduli of the eigenvalues of $\tilde{\mathbf{A}}$ by a small positive number δ (between 0·1 and 1) whenever these are lower than the number itself,[6] i.e. redefine

$$|\tilde{a}|^k_{j+1/2} = \begin{cases} |\tilde{a}|^k_{j+1/2} & \text{if } |\tilde{a}|^k_{j+1/2} > \delta, \\ \delta & \text{if } |\tilde{a}|^k_{j+1/2} \leqslant \delta. \end{cases} \tag{21}$$

A more refined treatment results if such correction is performed only when an unphysical jump is detected by means of the slope of the characteristics at that point.[7] These corrections can also be viewed as augmenting the numerical dissipation of the scheme to ensure entropy-satisfying (energy-dissipating in the case of the St. Venant equations) solutions. Other approaches have also been proposed by Sweby.[8]

SECOND-ORDER SCHEME

In this section corrections second-order in space and time are added to scheme (15), (16) based on the Lax–Wendroff numerical flux,[9] which can be written as

$$\mathbf{F}^{*\mathrm{LW}}_{j+1/2} = \tfrac{1}{2}(\mathbf{F}_{j+1} + \mathbf{F}_j) - \tfrac{1}{2}\mathbf{A}^2_{j+1/2}(\mathbf{U}_{j+1} - \mathbf{U}_j). \tag{22}$$

$\mathbf{A}_{j+1/2}$ is the Jacobian matrix (5) evaluated at some average of the variables at cells j and $j+1$. For instance, it could be defined as

$$\mathbf{A}_{j+1/2} = \mathbf{A}\left(\frac{\mathbf{U}_{j+1} + \mathbf{U}_j}{2}\right). \tag{23}$$

If the approximate Jacobian matrix $\tilde{\mathbf{A}}$ constructed in the previous section is used instead, numerical flux (22) can be reorganized as

$$\mathbf{F}^{*\mathrm{LW}}_{j+1/2} = \tfrac{1}{2}(\mathbf{F}_{j+1} + \mathbf{F}_j) - \tfrac{1}{2}\sum_{k=1}^{2} \tilde{\alpha}^k_{j+1/2}|\tilde{a}^k_{j+1/2}|\tilde{\mathbf{e}}^k_{j+1/2} + \tfrac{1}{2}\sum_{k=1}^{2} \tilde{\alpha}^k_{j+1/2}|\tilde{a}^k_{j+1/2}|(1 - \lambda|\tilde{a}^k_{j+1/2}|)\tilde{\mathbf{e}}^k_{j+1/2}, \tag{24}$$

which can be viewed as the first-order upwind numerical flux (16) plus a correction term. Following Roe[9] and Sweby,[10] one can limit this correction in order to obtain an oscillation-free second-order method, referred to as the Roe–Sweby scheme in the rest of this paper. Its numerical flux is then

$$\mathbf{F}^{*\mathrm{RS}}_{j+1/2} = \tfrac{1}{2}(\mathbf{F}_{j+1} + \mathbf{F}_j) - \tfrac{1}{2}\sum_{k=1}^{2} \tilde{\alpha}^k_{j+1/2}|\tilde{a}^k_{j+1/2}|\mathbf{e}^k_{j+1/2}$$
$$+ \tfrac{1}{2}\sum_{k=1}^{2} \varphi(r^k_{j+1/2})\tilde{\alpha}^k_{j+1/2}|\tilde{a}^k_{j+1/2}|(1 - \lambda|\tilde{a}^k_{j+1/2}|)\tilde{\mathbf{e}}^k_{j+1/2}. \tag{25}$$

The limiter φ in (25) is responsible for obtaining non-oscillatory solutions despite the presence of strong gradients or shocks. It is a non-linear function of the ratio

$$r^k_{j+1/2}=\frac{\tilde{\alpha}^k_{j+1/2-S}}{\tilde{\alpha}^k_{j+1/2}}, \qquad s=\text{sign}(\tilde{a}^k_{j+1/2}). \tag{26}$$

Several actual functional dependences on the r's that guarantee second-order accuracy (in space and time) as well as monotonicity are available in the literature. Among them the Superbee limiter is defined as

$$\varphi(r)=\max[0, \min(2r, 1), \min(r, 2)] \tag{27}$$

and the Van Leer limiter as

$$\varphi(r)=\frac{r+|r|}{1+r}. \tag{28}$$

The effect is basically the same for all of them and consists of limiting the amount of second-order correction added to the first-order scheme in regions of steep gradients of the flow.

NUMERICAL RESULTS

In order to asses the performance of the scheme presented in this paper for actual channel flow calculations, several test cases were computed. All the examples consider either rectangular or trapezoidal channels of a flat bed with no friction. Comparisons with the exact solution, when available, and with results from two other classical difference schemes (McCormack and Lax–Friedrichs) are shown.

Idealized dam-break problem

The first situation is supposed to simulate the catastrophic failure of a dam. In a channel 1000 m long, two different heights of still water are separated by a dam. At $t=0$ the dam is instantaneously removed, then a negative wave moves upstream and a surge rushes downstream. For the case of a rectangular channel there exists an exact solution based on the theory of characteristics.[11] Depending on the height ratio at the initial instant, the flow regime ranges from subcritical to strongly supercritical downstream of the dam location. In the case where supercritical flow is attained, the water remains critical at the dam site. This problem, although somewhat idealized, is very interesting to test the shock-capturing ability of the method.

The case shown in Figure 1 corresponds to a rectangular channel with an initial height ratio of 100, which leads to supercritical flow with a maximum Froude number ($Fr=u/c$) of 2·8 behind the surge. The depth ratio of the surge is 17. These can be considered as extremely exacting conditions for the difference scheme. Water depth and velocity, compared with the exact solution, for the three different numerical schemes are shown at a time in which the waves have not yet reached the boundaries of the computational domain ($t=8{\cdot}8$ s). All three were run at a CFL number of 0·95 and the channel was discretized with 101 points.

Figures 1(a) and 1(b) correspond to the Roe–Sweby scheme (water depth and velocity respectively). The Superbee limiting function (27) was used. The agreement with the exact solution can be considered as very good, the depression wave being correctly represented and the bore strength well predicted. Its position, however, is one mesh point behind the exact one.

Figures 1(c) and 1(d) show the results obtained with the McCormack scheme for the same conditions. This classical scheme is still widely used in computational hydraulics for its simplicity

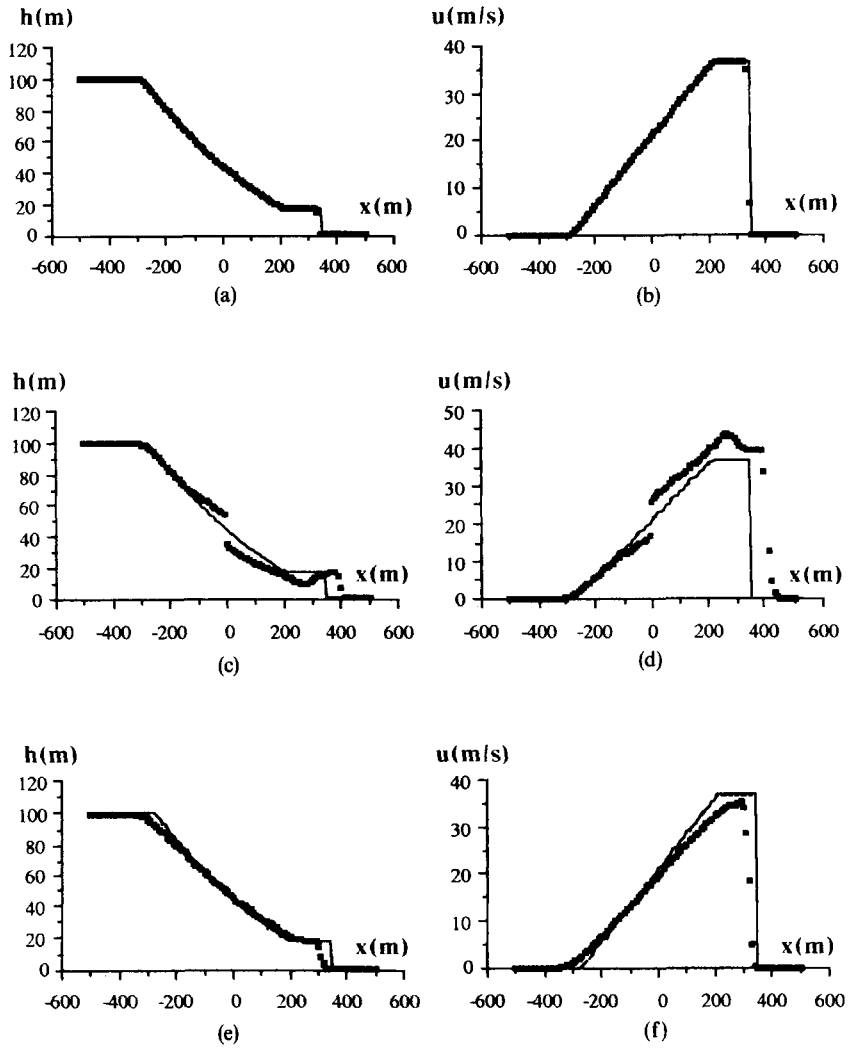

Figure 1. Idealized dam-break problem on rectangular channel at $t = 8{\cdot}8$ s. Solid line: exact solution. Dotted line: numerical solution. Left column represents water depth, right column represents flow velocity. (a), (b) Roe–Sweby scheme with Superbee limiter. (c), (d) McCormack scheme. (e), (f) Lax–Friedrichs scheme. All three run at CFL = 0·95 on 101 mesh points

and good performance even in the presence of discontinuities, though it does not cope well with complicated supercritical flows. Addition of artificial viscosity terms was needed in order to compute a stable solution, but still no satisfactory results could be obtained. An unphysical stationary jump appears at the dam location that spoils the solution. The front height is surprisingly well computed but its velocity is mispredicted.

The Lax–Friedrichs scheme was used to compute the results shown in Figures 1(e) and 1(f). As a first-order scheme it is too diffusive and leads to a strong smearing of the discontinuities present in the solution. However, it does not exhibit the unphysical jump of McCormack's method nor spurious oscillations, as corresponds to a monotone scheme.

It can be concluded that for this test case the Roe–Sweby scheme with the approximate Jacobian developed in a previous section can provide more accurate results than other classical methods. However, the computational cost is almost doubled. Optimization of the research code used to run these tests would perhaps improve the computational efficiency of the upwind scheme.

The same problem was run for a trapezoidal channel 1 m wide at the bottom with a lateral wall slope of unity. The initial conditions were the same as before, as were the CFL number and the number of mesh points. Although no exact solution is available for this problem, the main features of the flow can be drawn from the numerical solution, which is shown in Figures 2(a) and 2(b) (water depth and velocity respectively). Again a depression wave moves upstream while a surge wave travels downstream of the channel. It is to be remarked that, owing to the different geometry, the bore travels almost 1·5 times faster than for a rectangular channel (for this reason the solution at 7·6 s after dam removal was chosen) but is still well captured in only one mesh point. The numerical solution shows up stable and well behaved everywhere even though the Froude number behind the shock is in this case 7·4.

Bore propagation

An interesting test case is that of a bore propagating over another one. In a 1000 m long trapezoidal channel of the same shape as that of Figure 2 a bore of 1·94 m total height propagates over still water 1 m deep. Then another bore of 3·1 m total height is introduced above the first one. The latter travels faster and, consequently, at a time long enough will catch up with the former. The initial distribution of depth of water can be seen in Figure 3(a). This problem can show the ability of a method to capture discontinuities. The time increment is calculated every time step to fulfil the CFL condition for the largest wave speed in the domain of integration; therefore at points where the wave speed is smaller than the maximum, the effective CFL number is much lower. Thus the numerical results may deteriorate.

This effect can be seen in Figures 3(c) and 3(d). The McCormack scheme captures the first big jump well but oscillations appear at the second small one. The Lax–Friedrichs scheme is more severely affected, and while the first jump is still resolved, the second is completely smeared out. Figure 3(b) shows the results obtained with the Roe–Sweby scheme with the Superbee limiter (27). They follow closely the exact slution and both hydraulic jumps are captured in only one mesh point without any overshoot or undershoot. The CFL number of the calculation was 0·95 and 101 mesh points were used.

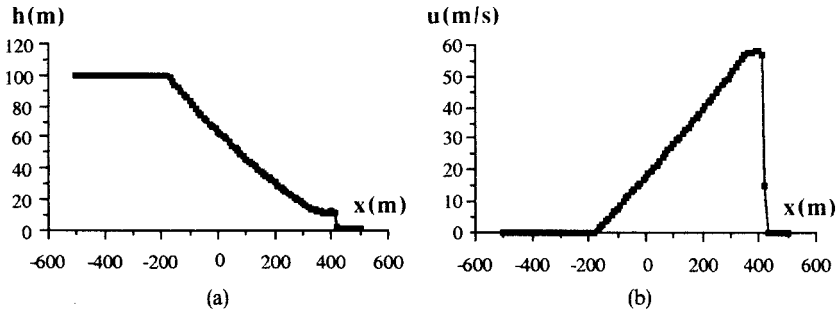

Figure 2. Idealized dam-break problem on a trapezoidal channel. Numerical solution obtained with Roe–Sweby scheme with Superbee limiter at $t = 7{\cdot}6$ s; CFL = 0·95, 101 mesh points

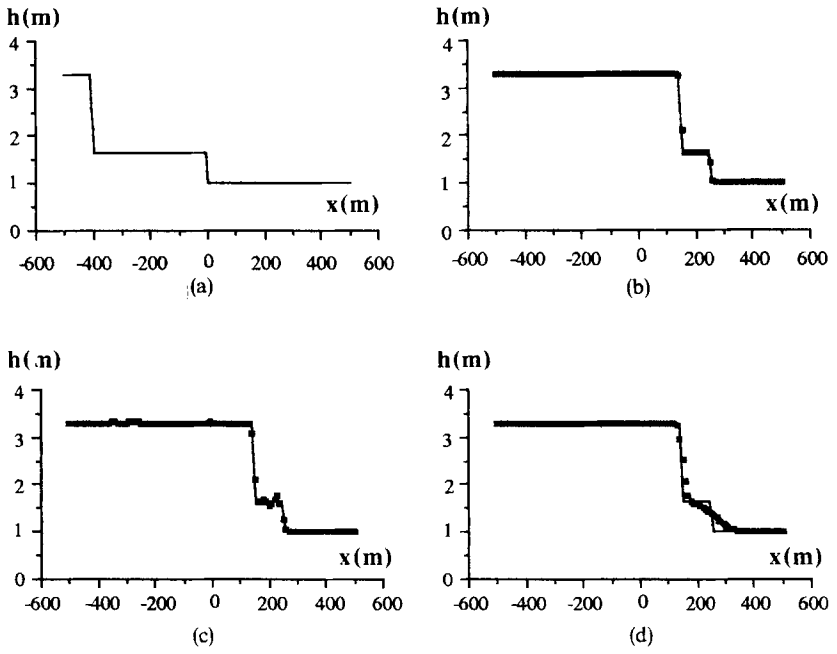

Figure 3. Bore propagation test case. Solid line: exact solution. Dotted line: numerical solution. (a) Initial water depth distribution. (b) Roe–Sweby scheme with Superbee limiter. (c) McCormack scheme. (d) Lax–Friedrichs scheme. All of them after 60 s at CFL = 0·95 on 101 mesh points

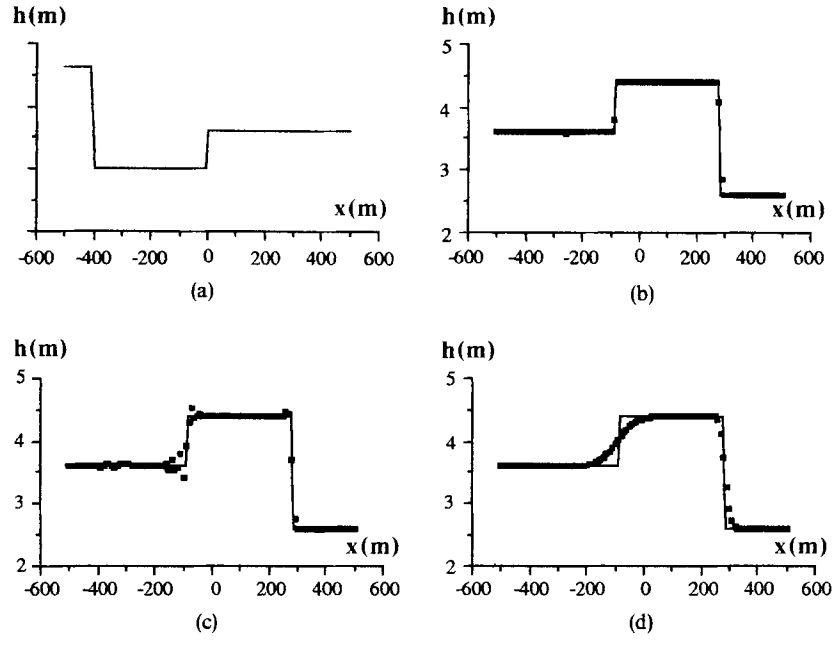

Figure 4. Bore interaction problem. Solid line: exact solution. Dotted line: numerical solution. (a) Initial water depth distribution. (b) Roe–Sweby scheme with Van Leer limiter. (c) McCormack scheme. (d) Lax–Friedrichs scheme. Results obtained at $t = 90$ s, CFL = 0·95 on 101 mesh points

Bore interaction

Finally, the interaction of two surge waves in a channel of the same characteristics was considered. It was computed at a CFL number of 0·95 with 101 mesh points. A bore 3·6 m deep of 100 $m^3 s^{-1}$ ($Fr = 1·34$) propagates downstream over water 2 m deep flowing at a rate of 10 $m^3 s^{-1}$ ($Fr = 0·5$). The downstream end is closed from the beginning so that a reflected wave 2·6 m deep travels upstream. The situation at time $t = 0$ can be seen in Figure 4(a).

When they meet, the result is two new surges travelling in reversed directions from a zone of 4·4 m deep water flowing at 103 $m^3 s^{-1}$ that forms and starts widening. The new created surge on the left is almost stationary; the front on the right travels downstream at 7 $m s^{-1}$. The exact solution can be obtained by solving the non-linear system of equations that results from applying the principles of conservation of mass and momentum in the channel just before and after the interaction. Numerical results to be compared with the exact water depth distribution after the meeting has taken place are shown in Figures 4(b)–4(d), which correspond to $t = 90$ s. Figure 4(b) displays the solution from the Roe–Sweby scheme with the Van Leer limiter (28). The agreement is very good, jumps being exactly represented in strength and position and captured in only one or at most two mesh points. The McCormack method (Figure 4(c)) shows an oscillating solution around the first jump and an overshoot in the second one. In Figure 4(d) it can be seen that Lax–Friedrichs scheme again tends to smear out both discontinuities, but mainly the small one.

CONCLUSIONS

A high-resolution scheme based on flux difference splitting and limiters is presented for the solution of open channel flow problems. An approximate Jacobian of the flux function is constructed that allows conservative upwind discretization of the equations for arbitrary shapes of the channel cross-section. This treatment enables efficient calculation of supercritical as well as subcritical flows and accurate capturing of rapidly rushing bores. Numerical experiments on idealized channel flow configurations show that the present method can cope better with complex supercritical flows than other classical schemes. Although the computational cost and complexity are higher than for more classical methods, the improvement in the solution appears worthwhile, especially for the most exacting flow conditions.

REFERENCES

1. P. L. Roe, 'A survey on upwind differencing techniques', *Lecture Series in CFD*, Von Karman Institute for Fluid Dynamics, 1989.
2. Ch. Hirsch, *Numerical Computation of Internal and External Flows, Vol. 2, Computational Methods for Inviscid and Viscous Flows*, Wiley, Chichester, 1990.
3. P. Glaister, 'Approximate Riemann solutions of the shallow water equations', *J. Hydraul. Res.*, **26**, 293–306 (1988).
4. J. A. Cunge, F. M. Holly and A. Verwey, *Practical Aspects of Computational River Hydraulics*, Pitman, London, 1980.
5. P. L. Roe, 'Approximate Riemann solvers, parameter vectors and difference schemes', *J. Comput. Phys.*, **43**, 357–372 (1981).
6. H. C. Yee, 'A class of high-resolution explicit and implicit shock-capturing methods', *NASA -TM 101088*, 1989.
7. A. Harten and P. Hyman 'Self adjusting grid methods for one-dimensional hyperbolic conservation laws', *J. Comput. Phys.*, **50**, 235–269 (1982).
8. P. K. Sweby, 'A modification of Roe's scheme for entropy satisfying solutions of scalar non-linear conservation laws', *Numerical Analysis Report*, University of Reading, 1982.
9. P. L. Roe, 'Efficient construction and utilisation of approximate Riemann solutions', in R. Glowinski (ed.), *Computing Methods in Applied Sciences and Engineering*, North-Holland, Amsterdam, 1984, pp. 499–518.
10. P. K. Sweby, 'High resolution schemes using flux limiters for hyperbolic conservation laws', *SIAM J. Numer. Anal.*, **21**, (1984).
11. J. J. Stoker, *Water Waves*, Interscience, New York, 1957.